

Baryonic Flux in Quenched and Two-Flavor Dynamical QCD

**V.G. Bornyakov,^{a,b,c} H. Ichie,^a Y. Mori,^a D. Pleiter,^d M.I. Polikarpov,^c
 G. Schierholz,^{d,e} T. Streuer,^{d,f} H. Stüben,^g and T. Suzuki^a**

^a*Institute for Theoretical Physics, Kanazawa University, Kanazawa 920-1192, Japan*

^b*Institute for High Energy Physics IHEP, 142284 Protvino, Russia*

^c*Institute of Theoretical and Experimental Physics ITEP, 117259 Moscow, Russia*

^d*John von Neumann-Institut für Computing NIC,
 Deutsches Elektronen-Synchrotron DESY, 15738 Zeuthen, Germany*

^e*Deutsches Elektronen-Synchrotron DESY, 22603 Hamburg, Germany*

^f*Institut für Theoretische Physik, Freie Universität Berlin, 14196 Berlin, Germany*

^g*Konrad-Zuse-Zentrum für Informationstechnik Berlin ZIB, 14195 Berlin, Germany*

– DIK Collaboration –

ABSTRACT: We study the distribution of color electric flux of the three-quark system in quenched and full QCD (with $N_f = 2$ flavors of dynamical quarks) at zero and finite temperature. To reduce ultra-violet fluctuations, the calculations are done in the abelian projected theory fixed to the maximally abelian gauge. In the confined phase we find clear evidence for a Y-shape flux tube surrounded and formed by the solenoidal monopole current, in accordance with the dual superconductor picture of confinement. In the deconfined, high temperature phase monopoles cease to condense, and the distribution of the color electric field becomes Coulomb-like.

1. Introduction

So far most investigations of the static potential, and the dynamics that drives it, have concentrated on the quark-antiquark ($Q\bar{Q}$) system, while little is known about the forces of the three-quark ($3Q$) ensemble. For understanding the structure of baryons and, in particular, for modelling the nucleon [1], it is important to learn about the forces and the distribution of color electric flux in the $3Q$ system as well. A particularly interesting question is whether a genuine three-body force exists and the confining flux tube is of Y-shape, or whether the long-range potential is simply the sum of two-body potentials, resulting in a flux tube of Δ -shape.

Several lattice studies report evidence for a Δ -type long-range potential [2, 3], while others claim a genuine three-body force [4, 5]. The latter result is also being supported by the cumulant expansion [6]. The difference between a Δ - and Y-shape potential is rather small and difficult to detect, because the underlying Wilson loop decays approximately exponentially with increasing interquark distance. A computation of the distribution of the color electric flux inside the baryon might help to resolve this problem.

In this paper we shall study the static potential and the flux tube of the $3Q$ system. The long-distance physics appears to be predominantly abelian – being the result of a yet unresolved mechanism – and driven by monopole condensation. The use of abelian variables is an essential ingredient in our work, as it leads to a substantial reduction of the statistical noise. Preliminary results of this investigation have been reported in Ref. [7].

The paper is organized as follows. In Section 2 we describe the details of our simulation, including the correlation functions that we are going to compute. The results of the calculation are presented in Sections 3 and 4. Section 3 is devoted to the study of the $3Q$ system at zero temperature, while Section 4 deals with the finite temperature case. Finally, in Section 5 we conclude.

2. Simulation details

We employ the Wilson gauge field action throughout this paper. In our studies of full QCD we are using non-perturbatively $O(a)$ improved Wilson fermions,

$$S_F = S_F^{(0)} - \frac{i}{2} \kappa g c_{SW} a^5 \sum_s \bar{\psi}(s) \sigma_{\mu\nu} F_{\mu\nu}(s) \psi(s), \quad (2.1)$$

with $N_f = 2$ flavors of dynamical quarks, where $S_F^{(0)}$ is the ordinary Wilson fermion action. Further details of the dynamical runs are given in [8, 9].

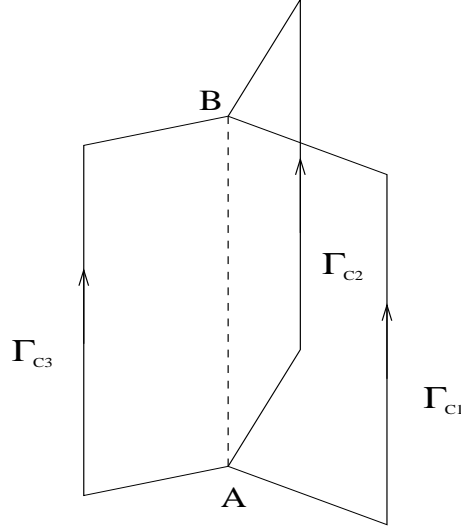


Figure 1: Three quark Wilson loop.

The system of three static quarks propagating from A to B may be described by the ‘baryonic’ Wilson loop

$$W_{3Q} = \frac{1}{3!} \varepsilon_{ijk} \varepsilon_{i'j'k'} U_{ii'}(\mathcal{C}_1) U_{jj'}(\mathcal{C}_2) U_{kk'}(\mathcal{C}_3), \quad (2.2)$$

where

$$U(\mathcal{C}) = \prod_{s, \mu \in \mathcal{C}} U(s, \mu) \quad (2.3)$$

is the ordered product of link matrices $U \in SU(3)$ along the path \mathcal{C} , as shown in Fig. 1. The potential energy of this system is given by

$$V = -\frac{1}{L_T} \lim_{L_T \rightarrow \infty} \log \langle W_{3Q} \rangle, \quad (2.4)$$

L_T being the temporal extent of the loop.

In the following we shall concentrate on abelian variables, referring to the maximally abelian gauge (MAG), and being obtained by standard abelian projection [10, 11]. To fix the MAG [12], we use a simulated annealing algorithm described in [9]. We write the abelian link variables as

$$u(s, \mu) \equiv \text{diag}(u_1(s, \mu), u_2(s, \mu), u_3(s, \mu)), \quad u_i(s, \mu) = \exp(i \theta_i(s, \mu)) \quad (2.5)$$

with

$$\theta_i(s, \mu) = \arg(U_{ii}(s, \mu)) - \frac{1}{3} \sum_{j=1}^3 \arg(U_{jj}(s, \mu)) \big|_{\text{mod } 2\pi} \in \left[-\frac{4}{3}\pi, \frac{4}{3}\pi\right]. \quad (2.6)$$

They take values in $U(1) \times U(1)$, and under a general gauge transformation they transform as

$$\begin{aligned} u(s, \mu) &\rightarrow d(s)^\dagger u(s, \mu) d(s + \hat{\mu}), \\ d(s) &= \text{diag}(\exp(i\alpha_1(s)), \exp(i\alpha_2(s)), \exp(-i(\alpha_1(s) + \alpha_2(s)))) . \end{aligned} \quad (2.7)$$

The abelian Wilson loop is given by

$$W_{3Q}^{\text{ab}} = \frac{1}{3!} |\varepsilon_{ijk}| u_i(\mathcal{C}_1) u_j(\mathcal{C}_2) u_k(\mathcal{C}_3), \quad (2.8)$$

where $u(\mathcal{C})$ is the abelian counterpart of (2.3). W_{3Q}^{ab} is invariant under gauge transformations (2.7).

The physical properties of the $3Q$ system can be inferred from correlation functions of appropriate operators with the corresponding Wilson loop. Abelian operators take the form

$$\mathcal{O}(s) = \text{diag}(\mathcal{O}_1(s), \mathcal{O}_2(s), \mathcal{O}_3(s)) \in U(1) \times U(1). \quad (2.9)$$

For C-parity even operators \mathcal{O} , like the action and monopole densities, the correlator of $\mathcal{O}(s)$ with the abelian Wilson loop is given by [13, 7]

$$\langle \mathcal{O}(s) \rangle_{3Q} = \frac{\langle \mathcal{O}(s) W_{3Q}^{\text{ab}} \rangle}{\langle W_{3Q}^{\text{ab}} \rangle} - \langle \mathcal{O} \rangle. \quad (2.10)$$

For C-parity odd operators, like the electric field and monopole current which carry a color index, the correlator is defined by

$$\langle \mathcal{O}(s) \rangle_{3Q} = \frac{1}{3!} \frac{\langle \mathcal{O}_i(s) |\varepsilon_{ijk}| u_i(\mathcal{C}_1) u_j(\mathcal{C}_2) u_k(\mathcal{C}_3) \rangle}{\langle W_{3Q}^{\text{ab}} \rangle}, \quad (2.11)$$

where summation over i, j, k is assumed. At finite temperature we will use the product P_{3Q} of three Polyakov loops closed around the boundary as baryonic source instead of W_{3Q} :

$$P_{3Q}^{\text{ab}} = \frac{1}{3!} |\varepsilon_{ijk}| \ell_i(\vec{s}_1) \ell_j(\vec{s}_2) \ell_k(\vec{s}_3), \quad (2.12)$$

where

$$\ell(\vec{s}) = \prod_{s_4=1}^{L_T} u(\vec{s}, s_4, 4) \quad (2.13)$$

is the abelian Polyakov loop, L_T being the temporal extent of the lattice here. The correlators of $\mathcal{O}(s)$ with P_{3Q} are defined analogously to (2.10) and (2.11).

The observables we shall study are the action density ρ_A^{3Q} , the color electric field E_i^{3Q} and the monopole current k^{3Q} . The action density is given by

$$\rho_A^{3Q}(s) = \frac{\beta}{3} \sum_{i, \mu > \nu} \langle \cos(\theta_i(s, \mu, \nu)) \rangle_{3Q}, \quad (2.14)$$

where

$$\begin{aligned}\theta_i(s, \mu, \nu) &= \arg(u_i(s, \mu, \nu)), \\ u_i(s, \mu, \nu) &= u_i(s, \mu)u_i(s + \hat{\mu}, \nu)u_i^\dagger(s + \hat{\nu}, \mu)u_i^\dagger(s, \nu)\end{aligned}\quad (2.15)$$

is the plaquette angle. The color electric field and monopole current correlators are defined by

$$E_i^{3Q}(s) = i \langle \text{diag}(\theta_1(s, 4, i), \theta_2(s, 4, i), \theta_3(s, 4, i)) \rangle_{3Q} \quad (2.16)$$

and

$$k^{3Q}(*s, \mu) = 2\pi i \langle \text{diag}(k_1(*s, \mu), k_2(*s, \mu), k_3(*s, \mu)) \rangle_{3Q}, \quad (2.17)$$

where $k_i(*s, \mu)$ is the monopole current [13, 9].

The calculations in full QCD at zero temperature are performed on the $24^3 48$ lattice at $\beta = 5.29$, $\kappa = 0.1355$, which corresponds to a pion mass of $m_\pi/m_\rho \approx 0.7$ and a lattice spacing of $a/r_0 = 0.18$ [9] (i.e. $a = 0.09$ fm assuming $r_0 = 0.5$ fm). The calculations in full QCD at finite temperature T are done on the $16^3 8$ lattice at $\beta = 5.2$ for various hopping parameters ranging from $\kappa = 0.1330$ to $\kappa = 0.1360$, which covers the temperature range [14] $0.8 \lesssim T/T_c \lesssim 1.2$. The critical temperature T_c corresponds to $\kappa = 0.1344(1)$. At this κ we find $m_\pi/m_\rho \approx 0.77$. For comparison, we also did quenched simulations at zero temperature on the $16^3 32$ lattice at $\beta = 6.0$. To reduce the statistical noise we smeared the spatial links of the abelian Wilson loop.

3. Static potential and baryonic flux at zero temperature

In Fig. 2 we show the baryon potential as a function of minimal Y-type distance between the quarks, i.e. the sum of the distance from the quarks to the Fermat point,

$$L_Y = \left(\frac{1}{2} \sum_{i>j} r_{ij}^2 + 2\sqrt{3} S_\Delta \right)^{1/2}, \quad (3.1)$$

where \vec{r}_i marks the position of the i^{th} quark, $r_{ij} = |\vec{r}_i - \vec{r}_j|$ and S_Δ is the area of the triangle spanned by the three quarks. An unphysical constant has been subtracted from the potentials. For equal distances between the quarks, i.e. $|\vec{r}_i - \vec{r}_j| = L_Y/\sqrt{3}$ for $\forall i \neq j$, we may fit the potential by

$$V(L_Y) = -3\sqrt{3} \frac{\alpha}{L_Y} + \sigma L_Y + V_0. \quad (3.2)$$

In the quenched approximation at $\beta = 6.0$ we obtain the abelian string tension $\sigma_{\text{ab}} a^2 = 0.038(1)$. Comparison of this value with the SU(3) result [4] gives $\sigma_{\text{ab}}/\sigma = 0.83(3)$, which lends further support to the hypothesis of abelian dominance. In Fig. 3 we compare the abelian potential in full and quenched QCD. We see that

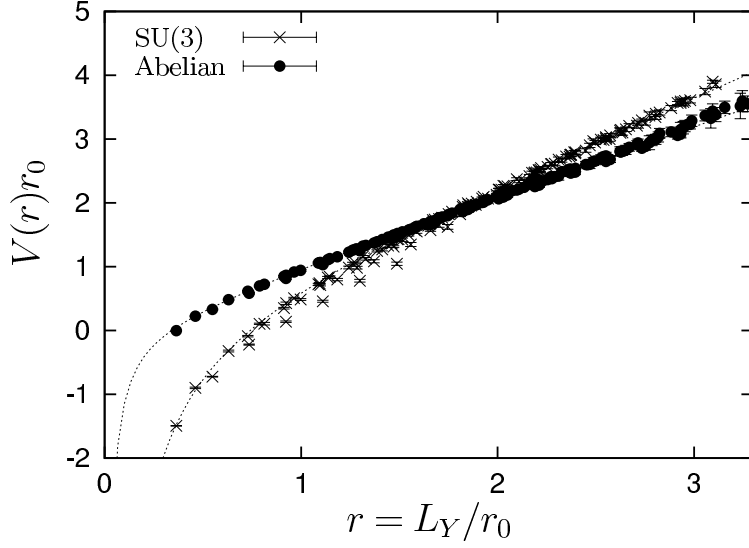


Figure 2: Comparison of the abelian and SU(3) baryon potential in the quenched approximation on the $16^3 32$ lattice at $\beta = 6.0$. The SU(3) potential is taken from [4].

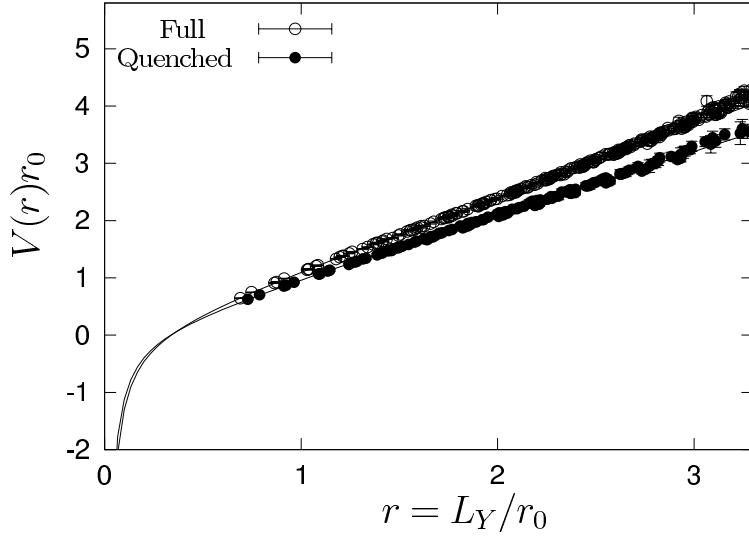


Figure 3: The abelian baryon potential in full and quenched QCD.

the abelian string tension in full QCD is slightly larger than the quenched value, a phenomenon which was already observed in case of the $Q\bar{Q}$ potential [9].

In Fig. 4 we show the distribution of the color electric field \vec{E}^{3Q} , and its surrounding monopole currents k^{3Q} , on the $24^3 48$ lattice in full QCD. The time direction

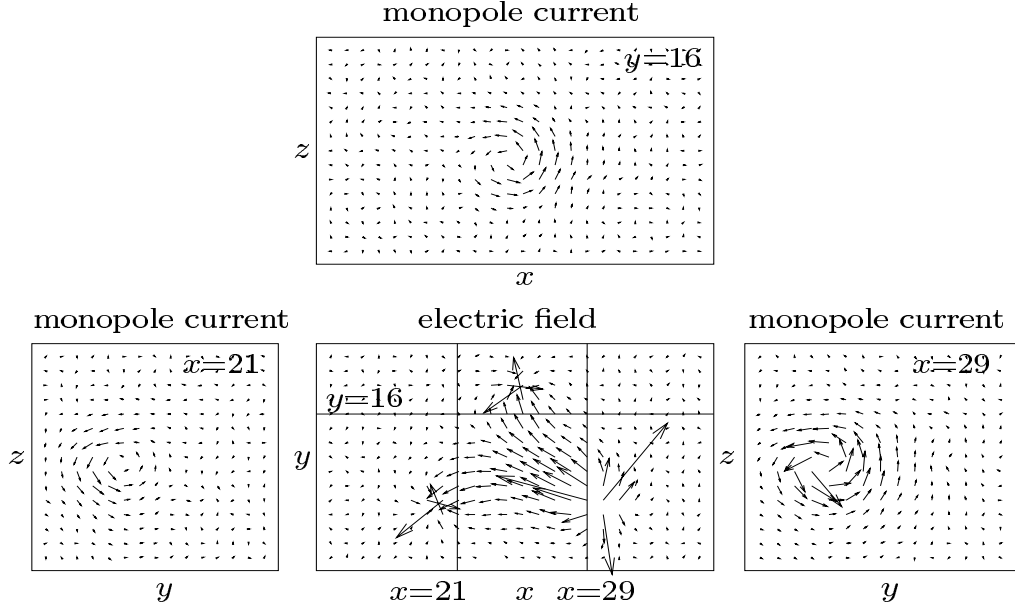


Figure 4: Distribution of the color electric field \vec{E}^{3Q} in the (x, y) plane on the $24^3 48$ lattice (center bottom figure), together with the monopole currents k^{3Q} in the (x, z) and (y, z) planes (adjacent figures), respectively, at the position marked by the respective solid lines. The magnitude of E^{3Q} and k^{3Q} is indicated by the length of the arrows.

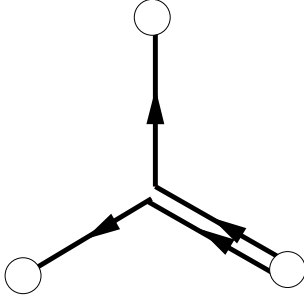


Figure 5: Schematic view of the color electric field.

of the Wilson loop has been taken in one of the spatial directions of the lattice. Points on the hyperplane orthogonal to the time direction of the Wilson loop are marked by (x, y, z) . The static quarks are placed at $(x, y, z) = (20, 10, 8)$, $(25, 18, 8)$ and $(30, 10, 8)$, respectively, i.e. they lie in the (x, y) plane. The color index of the electric field operator (cf. eq. (2.16)) is identified with the color index of the quark in the bottom-right corner (in the center bottom figure). Note that the sum of the electric field over the three color indices vanishes at any point. As expected, the flux

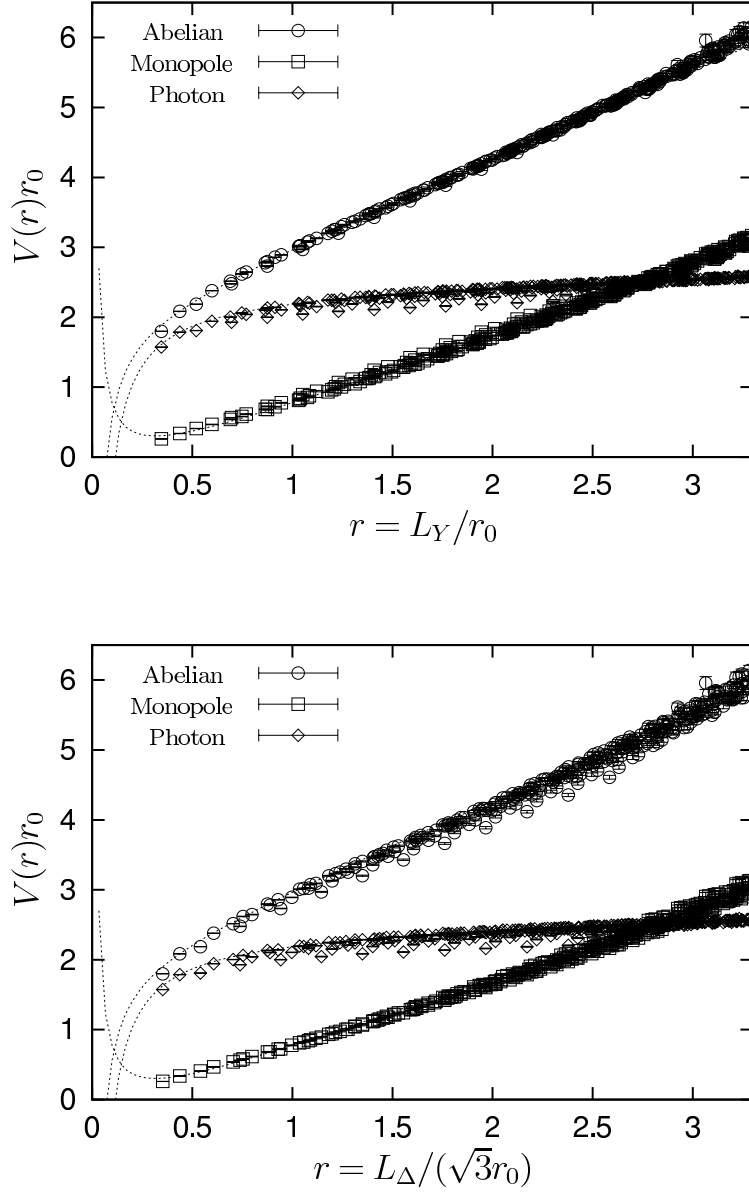


Figure 6: The abelian baryon potential in full QCD, together with its monopole and photon part, as a function of L_Y (top) and L_Δ (bottom), respectively.

emanates from the quark in the bottom-right corner and at about the center of the $3Q$ system splits into two parts. The flux lines are schematically drawn in Fig. 5. A similar picture holds for the top and bottom-left quark and their respective fluxes. In the adjacent figures we show the monopole current in the planes perpendicular to the electric flux lines, i.e. the (x, z) and (y, z) planes. They form a solenoidal current, as in the case of the $Q\bar{Q}$ system, in agreement with the dual superconductor picture of confinement.

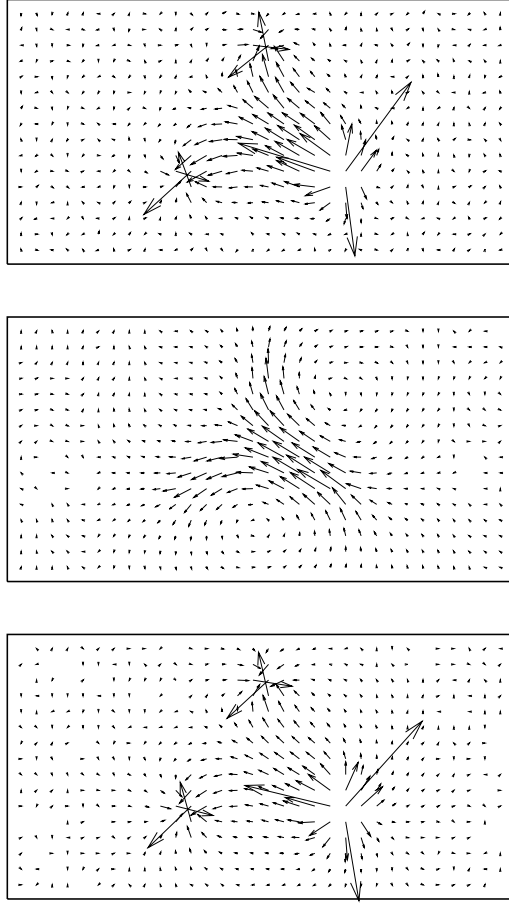


Figure 7: Distribution of the abelian color electric field \vec{E}^{3Q} (top) broken into monopole (middle) and photon parts (bottom) on the $24^3 48$ lattice in full QCD. The color index of the electric field operators corresponds to that of the quark in the bottom right corner. Only part of the lattice is shown here.

If the confining flux is of Y-shape we would expect the long-distance part of the potential to be a universal function of L_Y . In Fig. 6 we plot the abelian potential as a function of L_Y , and as a function of the perimeter of the triangle formed by the quarks

$$L_{\Delta} = \sum_{i < j} |\vec{r}_i - \vec{r}_j|. \quad (3.3)$$

The data show a universal behavior when plotted against L_Y . This is to a lesser extent the case when plotted against L_{Δ} , which supports a genuine three-body force

of Y-type. The fits in the bottom part of the figure were done using the ansatz

$$V(L_\Delta) = -9\frac{\alpha}{L_\Delta} + \frac{1}{\sqrt{3}}\sigma L_\Delta + V_0. \quad (3.4)$$

We may decompose the abelian gauge field into a monopole and photon part according to the definition [15, 16]

$$\begin{aligned} \theta_i(s, \mu) &= \theta_i^{\text{mon}}(s, \mu) + \theta_i^{\text{ph}}(s, \mu), \\ \theta_i^{\text{mon}}(s, \mu) &= 2\pi \sum_{s'} D(s - s') \nabla_\alpha^{(-)} m_i(s', \alpha, \mu), \end{aligned} \quad (3.5)$$

where $D(s) = \Delta^{-1}(s)$ is the lattice Coulomb propagator, $\nabla_\mu^{(-)}$ is the lattice backward derivative, and $m_i(s, \mu, \nu)$ counts the number of Dirac strings piercing the plaquette $u_i(s, \mu, \nu)$. If one computes $k_i(*s, \mu)$ from $\theta_i^{\text{mon}}(s, \mu)$ one recovers almost all monopole currents. In Fig. 6 we see that the monopole part is largely responsible for the linear behavior of the potential, as was found already in case of the $Q\bar{Q}$ potential [9]. The ratio of monopole to abelian string tension turns out to be 0.81(3).

In Fig. 7 we show the distribution of the abelian color electric field \vec{E}^{3Q} on the $24^3 48$ lattice in full QCD, broken into monopole and photon parts. The photon part shows a Coulomb-like distribution, while the monopole part has no sources. Outside the flux tube the monopole and photon parts of the color electric field largely cancel. The middle figure shows clearly that the flux lines are attracted to a Y-type geometry.

In Fig. 8 we show the action density ρ_A^{3Q} of the $3Q$ system in full QCD. Also shown is the monopole and photon part of ρ_A^{3Q} separately. Let us first look at the (full) abelian density. It clearly displays a Y-type geometry of the color forces. This is, of course, indistinguishable from a geometry of purely two-body forces with strongly attracting flux lines. The monopole part of the action density shows no sources. Apart from that, it appears that the action density originates almost entirely from the monopole part. The sources show up in the photon part of the action density as expected.

We have done similar calculations (to the ones shown in Figs. 4 – 8) in quenched QCD as well. Part of our findings have been reported in [7], and we refrain from repeating them here. Qualitatively, we found the same results as in full QCD at $m_\pi/m_\rho \approx 0.7$.

4. Baryonic flux at finite temperature

We expect the flux tube to disappear and the color electric field to become Coulomb- or Yukawa-like above the finite temperature phase transition T_c and when the string breaks in full QCD. This phenomenon has been observed in case of the $Q\bar{Q}$ system in the pure SU(2) gauge theory for temperatures $T > T_c$ [17] and in full QCD for T just below and above T_c [18]. Throughout this Section we shall use the Polyakov loop (2.12) to create a baryon.

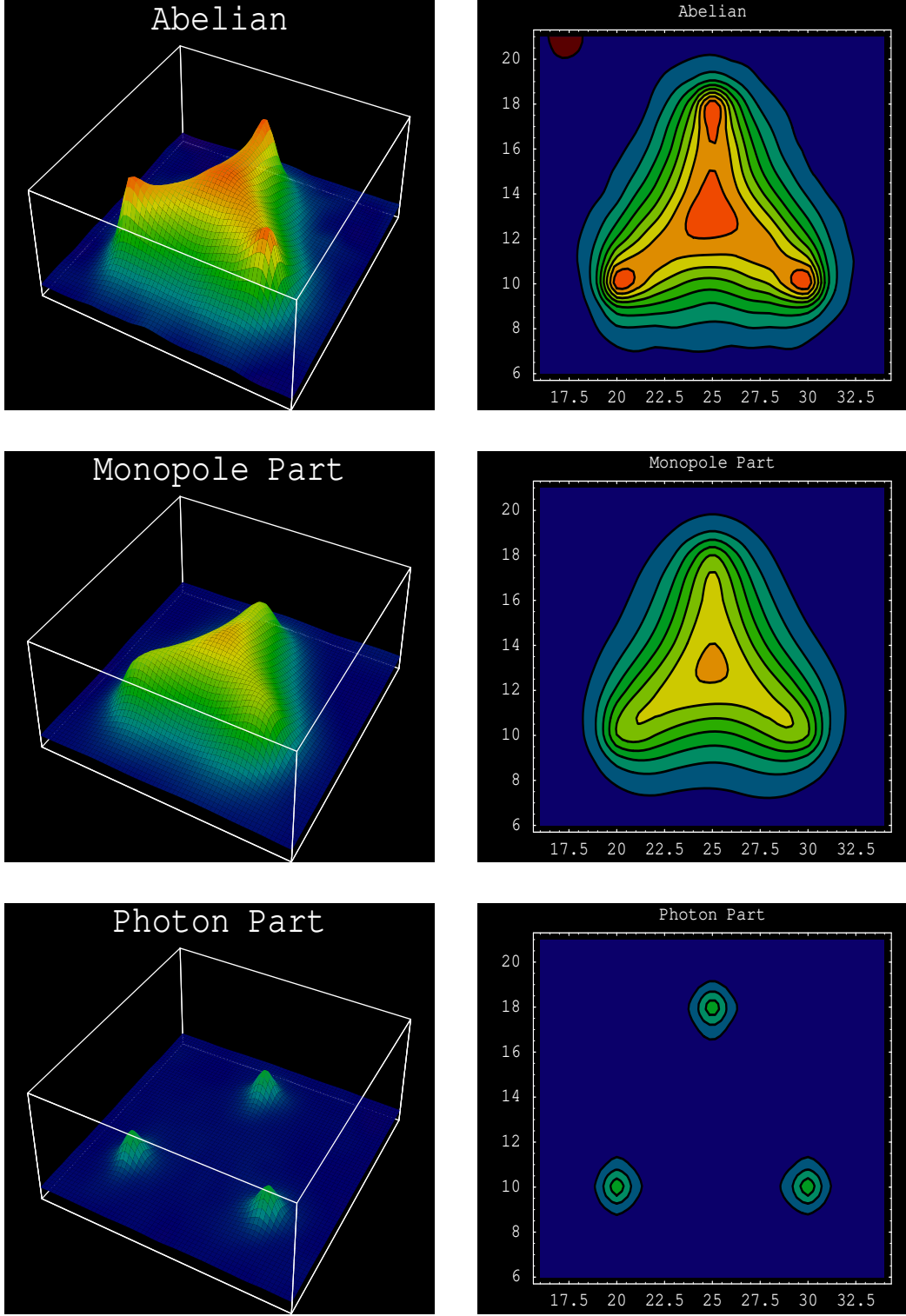


Figure 8: The abelian action density of the $3Q$ system in full QCD, together with the monopole and photon part.

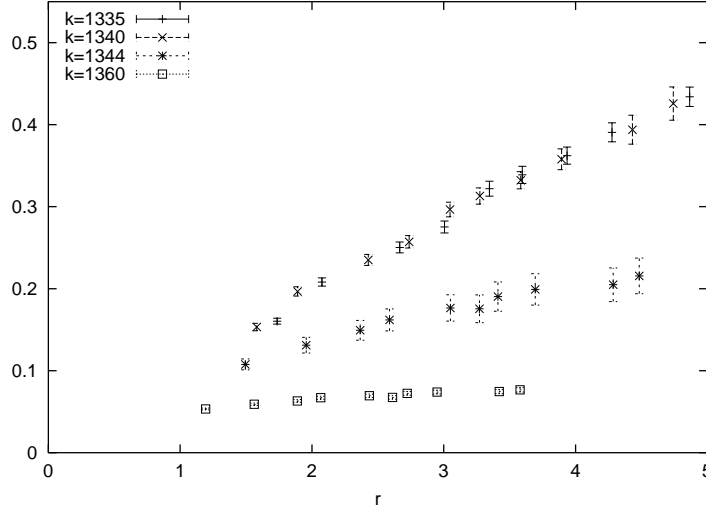


Figure 9: The monopole part of the baryon potential at finite temperature in full QCD as a function of L_V ($T < T_c$) and L_Δ ($T > T_c$), respectively, in units of *God knows what*.

In Fig. 9 we show the baryon potential on the $16^3 8$ lattice at $\beta = 5.2$ for several values of κ . At this β value

$$T \propto \exp(-2.81/\kappa). \quad (4.1)$$

Increasing κ thus increases the temperature. We cross the finite temperature phase transition at $\kappa = 0.1344$ [14]. We see that the potential flattens off while we approach the transition point. However, the distances we were able to probe are not large enough to make any statement about string breaking.

To compute the action density ρ_A^{3Q} and the electric field and monopole correlators E_i^{3Q} and k^{3Q} , respectively, we need to reduce the statistical noise. Note that the Polyakov loops span an area of $\approx 16 \times 8$ lattice spacings. We do that by using extended operators

$$\begin{aligned} \rho_A^{3Q}(s) \longrightarrow & \frac{1}{8} \{ \rho_A^{3Q}(s) + \rho_A^{3Q}(s - \hat{x} - \hat{y} - \hat{z}) + \rho_A^{3Q}(s - \hat{x} - \hat{y}) \\ & + \rho_A^{3Q}(s - \hat{x} - \hat{z}) + \rho_A^{3Q}(s - \hat{y} - \hat{z}) + \rho_A^{3Q}(s - \hat{x}) \\ & + \rho_A^{3Q}(s - \hat{y}) + \rho_A^{3Q}(s - \hat{z}) \}, \end{aligned} \quad (4.2)$$

$$\begin{aligned} E_i^{3Q}(s) \longrightarrow & \frac{1}{4} \{ E_i^{3Q}(s) + E_i^{3Q}(s - \hat{x} - \hat{t}) \\ & + E_i^{3Q}(s - \hat{x}) + E_i^{3Q}(s - \hat{t}) \}, \end{aligned} \quad (4.3)$$

$$k^{3Q}(s, \mu) \longrightarrow \frac{1}{2} \{ k^{3Q}(s, \mu) + k^{3Q}(s - \hat{z}, \mu) \}, \quad (4.4)$$

where (again) we have assumed that the quarks lie in the (x, y) plane, and we call the direction of the Polyakov lines the t direction.

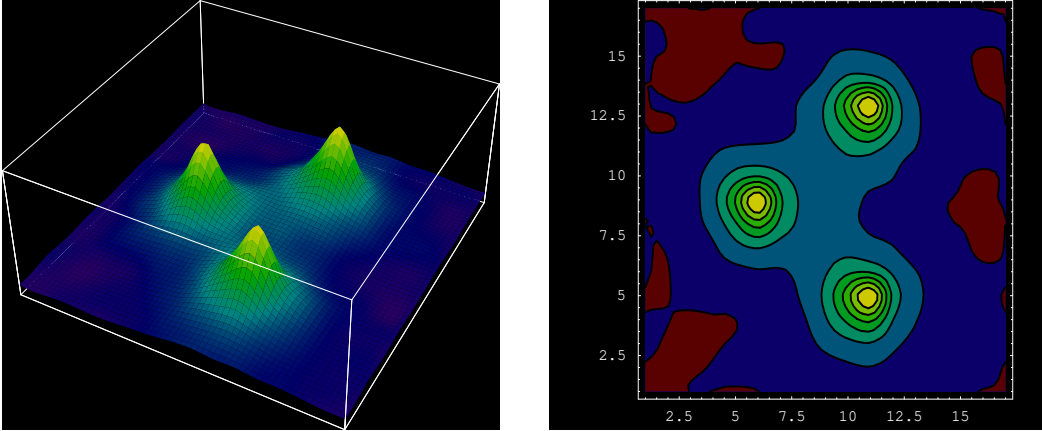


Figure 10: The Abelian action density in the deconfined phase at $\kappa = 0.1360$.

In Fig. 10 we plot the abelian action density in the deconfined phase at $\kappa = 0.1360$. As was to be expected, the action density shows three Coulomb-like peaks at the position of the quarks, similar to the photon part of the action density at zero temperature as shown in Fig. 8.

In Fig. 11 we show the monopole part of the electric field, averaged over the color components, and the accompanying monopole current for three values of κ , corresponding (from left to right) to the confined case, to $T \approx T_c$ and to the deconfined phase. In the confinement phase ($\kappa = 0.1335$) we find the flux to be of Y-shape, similar to the zero temperature case where we used Wilson loop correlators. Note that the Polyakov lines do not have a Y-shape junction like the Wilson loop does, which excludes the possibility that the flux is being induced by the color lines. Just below T_c ($\kappa = 0.1344$) we still see a Y-shape flux, while in the deconfined phase ($\kappa = 0.1360$) the electric field becomes Coulomb-like.

5. Conclusions

We have studied the $3Q$ system in the maximally abelian gauge in full QCD at zero and at finite temperature. Among the quantities we have looked at are the abelian baryon potential as well as the flux distribution and the action density. While on the basis of the potential it is hard to decide whether the long-range potential is of Δ - or Y-type, the distribution of the color electric field and the action density clearly shows a Y-shape geometry. As in the $Q\bar{Q}$ system, we identified the solenoidal monopole current to be responsible for squeezing the color electric flux into a narrow tube. Little difference to the quenched theory was found. In the deconfined phase the flux tube disappears, and the color electric field assumes a Coulomb-like form.

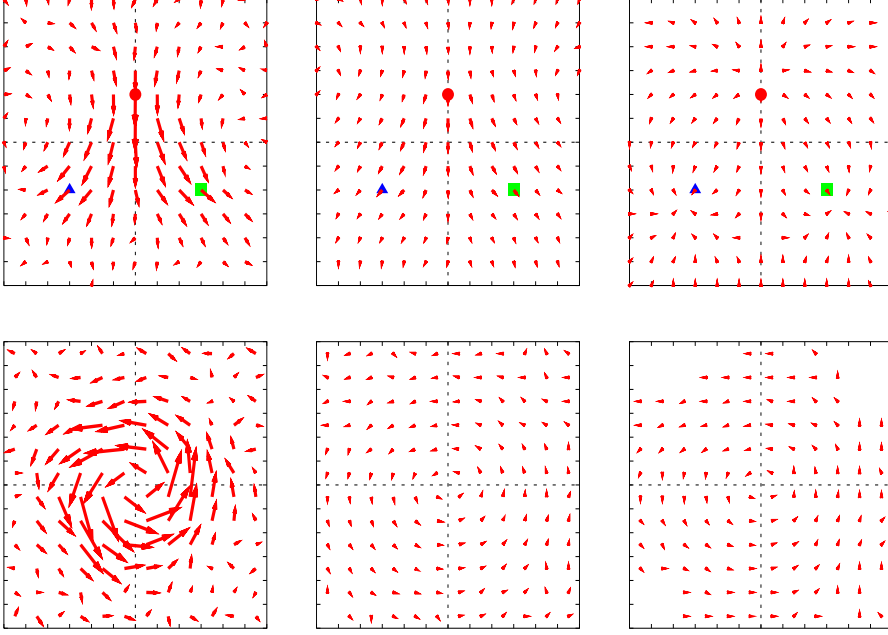


Figure 11: The color electric field (top) and monopole currents (bottom) on the $16^3 8$ lattice at $\kappa = 0.1335$ (left), 0.1344 (middle) and 0.1360 (right). The three quarks lie in (what we call) the (x, y) plane. The bottom figures show the monopole currents in the (x, z) plane at the position marked by the solid lines in the top figures.

Our results are in qualitative agreement with the predictions of the dual Ginzburg-Landau model [19].

Acknowledgements

The dynamical gauge field configurations at $T = 0$ have been generated on the Hitachi SR8000 at LRZ Munich. We thank the operating staff for their support. The dynamical gauge field configurations at $T > 0$ have been generated on the Hitachi SR8000 at KEK Tsukuba. The analysis has largely been done on the COMPAQ Alpha Server ES40 at Humboldt University, as well as on the NEC SX5 at RCNP Osaka. We wish to thank M. Müller-Preussker, Y. Koma and H. Suganuma for useful discussions. H.I. thanks the Humboldt University and Kanazawa University for hospitality. V.B. is supported by JSPS. T.S. is supported by JSPS Grant-in-Aid for Scientific Research on Priority Areas 13135210 and 15340073. M.I.P. is supported by grants RFBR 02-02-17308, RFBR 01-02-17456, INTAS-00-00111, DFG-RFBR 436RUS113/739/01, RFBR-DFG 03-02-04016 and CRDF award RPI-2364-MO-02.

References

- [1] S. Capstick and N. Isgur, Phys. Rev. D34 (1986) 2809.
- [2] G.S. Bali, Phys. Rep. 343 (2001) 1.
- [3] C. Alexandrou, Ph. de Forcrand and A. Tsapalis, Phys. Rev. D65 (2002) 054503.
- [4] T.T. Takahashi, H. Suganuma, Y. Nemoto and H. Matsufuru, Phys. Rev. D65 (2002) 114509; T.T. Takahashi, H. Matsufuru, Y. Nemoto and H. Suganuma, Phys. Rev. Lett. 86 (2001) 18.
- [5] C. Alexandrou, Ph. de Forcrand and O. Jahn, Nucl. Phys. (Proc. Suppl.) 119 (2003) 667.
- [6] D.S. Kuzmenko and Yu.A. Simonov, Phys. Lett. B494 (2000) 81; D.S. Kuzmenko and Yu.A. Simonov, [hep-ph/0302071](#).
- [7] H. Ichie, V. Bornyakov, T. Streuer and G. Schierholz, Nucl. Phys. (Proc. Suppl.) 119 (2003) 751; H. Ichie, V. Bornyakov, T. Streuer and G. Schierholz, Nucl. Phys. A721 (2003) 899.
- [8] H. Stüben, Nucl. Phys. (Proc. Suppl.) 94 (2001) 273.
- [9] V.G. Bornyakov, H. Ichie, Y. Koma, Y. Mori, Y. Nakamura, D. Pleiter, M.I. Polikarpov, G. Schierholz, T. Streuer, H. Stüben and T. Suzuki, [hep-lat/0310011](#).
- [10] G. 't Hooft, Nucl. Phys. B190 (1981) 455.
- [11] A.S. Kronfeld, M.L. Laursen, G. Schierholz and U.-J. Wiese, Phys. Lett. B198 (1987) 516.
- [12] F. Brandstaeter, G. Schierholz and U.-J. Wiese, Phys. Lett. B272 (1991) 319.
- [13] V. Bornyakov, H. Ichie, S. Kitahara, Y. Koma, Y. Mori, Y. Nakamura, M. Polikarpov, G. Schierholz, T. Streuer, H. Stüben and T. Suzuki, Nucl. Phys. (Proc. Suppl.) (2002) 634.
- [14] V.G. Bornyakov, M.N. Chernodub, H. Ichie, Y. Koma, Y. Mori, Y. Nakamura, M.I. Polikarpov, G. Schierholz, A. Slavnov, H. Stüben, T. Suzuki, P. Uvarov and V.I. Veselov, [hep-lat/040101403](#).
- [15] J. Smit and A. van der Sijs, Nucl. Phys. B355 (1991) 603.
- [16] T. Suzuki, S. Ilyar, Y. Matsubara, T. Okude and K.Yotsuji, Phys. Lett. B347 (1995) 375; Erratum: *ibid.* B351 (1995) 603.
- [17] Y. Peng and R.W. Haymaker, Phys. Rev. D52 (1995) 3030.
- [18] V. Bornyakov, H. Ichie, Y.Koma, Y. Mori, Y. Nakamura, M. Polikarpov, G. Schierholz, T. Streuer and T. Suzuki, Nucl. Phys. (Proc. Suppl.) 119 (2003) 712.

[19] Y. Koma, E.-M. Ilgenfritz, T. Suzuki, H. Toki, Phys. Rev. D64 (2001) 014015.